Electrically tunable microlens arrays based on polarization-independent optical phase of nano liquid crystal droplets dispersed in polymer matrix

Ji Hoon Yu,[1,4] Hung-Shan Chen,[3,4] Po-Ju Chen,[3,4] Ki Hoon Song,[1] Seong Cheol Noh,[1] Jae Myeong Lee,[1] Hongwen Ren,[2] Yi-Hsin Lin,[3,5] and Seung Hee Lee,[1,2,*]

[1]*Applied Materials Institute for BIN Convergence, Department of BIN Fusion Technology, Chonbuk National University, Jeonju, Jeonbuk, 561-756, South Korea*

[2]*Department of Polymer-Nano Science and Technology, Chonbuk National University, Jeonju, Jeonbuk, 561-756, South Korea*

[3]*Department of Photonics, National Chiao Tung University, 1001 Ta Hsueh Rd., Hsinchu 30010, Taiwan*

[4]*These authors contributed equally to this work*

[5]*yilin@mail.nctu.edu.tw*

[*]*lsh1@chonbuk.ac.kr*

Abstract: Electrically tunable focusing microlens arrays based on polarization independent optical phase of nano liquid crystal droplets dispersed in polymer matrix are demonstrated. Such an optical medium is optically isotropic which is so-called an optically isotropic liquid crystals (OILC). We not only discuss the optical theory of OILC, but also demonstrate polarization independent optical phase modulation based on the OILC. The experimental results and analytical discussion show that the optical phase of OILC microlens arrays results from mainly orientational birefringence which is much larger than the electric-field–induced birefringence (or Kerr effect). The response time of OILC microlens arrays is fast~5.3ms and the tunable focal length ranges from 3.4 mm to 3.8 mm. The potential applications are light field imaging systems, 3D integrating imaging systems and devices for augment reality.

OCIS codes: (160.3710) Liquid crystals; (230.2090) Electro-optical devices; (230.3720) Liquid-crystal devices.

References and links

1. O. Cakmakci and J. Rolland, "Head-worn displays: a review," J. Disp. Technol. **2**(3), 199–216 (2006).
2. B. Furht, *Handbook of augmented reality* (Springer, 2011).
3. H. Ren and S. T. Wu, *Introduction to adaptive lenses* (Wiley, 2012).
4. Y. H. Lin, H. S. Chen, H. C. Lin, Y. S. Tsou, H. K. Hsu, and W. Y. Li, "Polarizer-free and fast response microlens arrays using polymer-stabilized blue phase liquid crystals," Appl. Phys. Lett. **96**(11), 113505 (2010).
5. Y. H. Lin, H. Ren, Y. H. Wu, Y. Zhao, J. Fang, Z. Ge, and S. T. Wu, "Polarization-independent liquid crystal phase modulator using a thin polymer-separated double-layered structure," Opt. Express **13**(22), 8746–8752 (2005).
6. H. Ren, Y. H. Lin, and S. T. Wu, "Polarization-independent and fast-response phase modulators using double-layered liquid crystal gels," Appl. Phys. Lett. **88**(6), 061123 (2006).
7. M. Ye, B. Wang, and S. Sato, "Polarization-independent liquid crystal lens with four liquid crystal layers," IEEE Photon. Technol. Lett. **3**, 505–507 (2006).
8. D. K. Yang and S. T. Wu, *Fundamentals of Liquid Crystal Devices* (John Wiley, 2006).
9. Y. H. Lin and H. S. Chen, "Electrically tunable-focusing and polarizer-free liquid crystal lenses for ophthalmic applications," Opt. Express **21**(8), 9428–9436 (2013).
10. H. C. Lin and Y. H. Lin, "A fast response and large electrically tunable-focusing imaging system based on switching of two modes of a liquid crystal lens," Appl. Phys. Lett. **97**(6), 063505 (2010).
11. H. C. Lin and Y. H. Lin, "An electrically tunable focusing pico-projector adopting a liquid crystal lens," Jpn. J. Appl. Phys. **49**(10), 102502 (2010).

#240077 Received 30 Apr 2015; revised 8 Jun 2015; accepted 22 Jun 2015; published 24 Jun 2015

12. Y. H. Lin, M. S. Chen, and H. C. Lin, "An electrically tunable optical zoom system using two composite liquid crystal lenses with a large zoom ratio," Opt. Express **19**(5), 4714–4721 (2011).
13. H. C. Lin, N. Collings, M. S. Chen, and Y. H. Lin, "A holographic projection system with an electrically tuning and continuously adjustable optical zoom," Opt. Express **20**(25), 27222–27229 (2012).
14. Y. S. Tsou, Y. H. Lin, and A. C. Wei, "Concentrating photovoltaic system using a liquid crystal lens," IEEE Photon. Technol. Lett. **24**(24), 2239–2242 (2012).
15. H. S. Chen and Y. H. Lin, "An endoscopic system adopting a liquid crystal lens with an electrically tunable depth-of-field," Opt. Express **21**(15), 18079–18088 (2013).
16. X. Shen, Y. J. Wang, H. S. Chen, X. Xiao, Y. H. Lin, and B. Javidi, "Extended depth-of-focus 3D micro integral imaging display using a bifocal liquid crystal lens," Opt. Lett. **40**(4), 538–541 (2015).
17. H. Ren, Y. H. Lin, Y. H. Fan, and S. T. Wu, "Polarization-independent phase modulation using a polymer-dispersed liquid crystal," Appl. Phys. Lett. **86**(14), 141110 (2005).
18. Y. H. Lin, H. Ren, and S. T. Wu, "Polarisation-independent liquid crystal devices," Liq. Cryst. Today **17**(1-2), 2–8 (2008).
19. S. T. Wu and D. K. Yang, *Reflective Liquid Crystal Displays* (Wiley, 2001).
20. F. Basile, F. Bloisi, L. Vicari, and F. Simoni, "Optical phase shift of polymer-dispersed liquid crystals," Phys. Rev. E Stat. Phys. Plasmas Fluids Relat. Interdiscip. Topics **48**(1), 432–438 (1993).
21. Y. H. Lin and Y. S. Tsou, "A polarization independent liquid crystal phase modulation adopting surface pinning effect of polymer dispersed liquid crystals," J. Appl. Phys. **110**(11), 114516 (2011).
22. H. Ren, Y. H. Fan, Y. H. Lin, and S. T. Wu, "Tunable-focus microlens arrays using nanosized polymer-dispersed liquid crystal droplets," Opt. Commun. **247**(1-3), 101–106 (2005).
23. Y. Tanabe, H. Furue, and J. Hatano, "Optically isotopic liquid crystals with microsized domains," Mater. Sci. Eng. B **120**(1-3), 41–44 (2005).
24. J. W. Doane, N. A. Vaz, B. G. Wu, and S. Zumer, "Field controlled light-scattering from nematic microdroplets," Appl. Phys. Lett. **48**(4), 269–271 (1986).
25. R. Caputo, A. De Luca, L. De Sio, L. Pezzi, G. Strangi, C. Umeton, A. Veltri, R. Asquini, A. d'Alessandro, D. Donisi, R. Beccherelli, A. V. Sukhov, and N. V. Tabiryan, "POLICRYPS: a liquid crystal composed nano/microstructure with a wide range of optical and electro-optical applications," J. Opt. a-Pure. Appl. Opt. **11**, 024017 (2009).
26. V. P. Tondiglia, L. V. Natarajan, R. L. Sutherland, T. J. Bunning, and W. W. Adams, "Volume Holographic Image Storage and Electro-optical Readout in a Polymer-Dispersed Liquid-Crystal Film," Opt. Lett. **20**(11), 1325–1327 (1995).
27. T. J. Bunning, L. V. Natarajan, V. P. Tondiglia, and R. L. Sutherland, "Holographic polymer-dispersed liquid crystals(H-PDLCs)," Annu. Rev. Mater. Sci. **30**(1), 83–115 (2000).
28. J. Qi and G. P. Crawford, "Holographically formed polymer dispersed liquid crystal displays," Displays **25**(5), 177–186 (2004).
29. J. Niziol, R. Weglowski, S. J. Klosowicz, A. Majchrowski, P. Rakus, A. Wojciechowski, I. V. Kityk, S. Tkaczyk, and E. Gondek, "Kerr modulators based on polymer-dispersed liquid crystal complexes," J. Mater. Sci. Mater. Electron. **21**(10), 1020–1023 (2010).
30. H. S. Kitzerow, "Blue phase come of age: a review," Proc. SPIE **7232**, 723205 (2009).
31. Y. H. Lin, H. S. Chen, C. H. Wu, and H. K. Hsu, "Measuring electric-field-induced birefringence in polymer stabilized blue-phase liquid crystals based on phase shift measurements," J. Appl. Phys. **109**(10), 104503 (2011).

1. Introduction

Augmented reality (AR) is a technology to make people directly see the real-world environment augmented by computer-generated sensory information. Many companies and researchers are developing optical elements, sensors or systems for realizing wearable devices or head-mounted devices of AR [1,2]. The main structure of AR wearable devices consists of liquid crystal display (LCD) panel, projection lens modules and light guides. However, all the optical systems have internal aberrations due to manufacture and everyone has different eye conditions. In addition, the projected images from LCD panel have disadvantages of the color shift and degradation of gray level due to the dispersion of light guide or optical elements. As a result, it is required to develop electrically adaptive optical element to compensate the problems in order to tailor the AR systems to individual needs, such as tunable focusing liquid crystal (LC) lenses, LC lens arrays, liquid lenses/lens arrays, and spatial light modulators [3–7]. Liquid crystal (LC) lens arrays whose focal lengths are electrically tunable by spatial orientations of LC molecules under external electrical fields have advantages of light weight, simple optical designs, operations, and fabrications. Many structures of LC lenses have been proposed and so do the applications, such as integrating systems for 3D image, endoscopy, projection systems, and ophthalmic lenses [8–16]. The phase profile of the LC lens arrays can

#240077 Received 30 Apr 2015; revised 8 Jun 2015; accepted 22 Jun 2015; published 24 Jun 2015

be manipulated by designing distribution of external electric fields. However, many demerits of LC lens arrays are still needed to be improved, such as slow response time (~from few tens of ms to seconds) and low optical efficiency (<50%) due to the requirement of a polarizer, a small viewing angle limited by the polarizer, and low tolerance of thickness variation or low stiffness, which are not suitable for applications in touchscreens of portable devices. To overcome the obstacles, many researchers proposed polarizer-free LC lenses based on polarization independent LC phase modulations, such as double layered-type [5–7], residual phase types [17–22], and the type of blue phase liquid crystals (BPLC) based on Kerr effect [4]. T o solve the drawbacks of typical LC lens arrays, polymer dispersed liquid crystal (PDLC) consisting of LC droplets dispersed in polymer matrix is a good candidate among polarization independent LC phase modulations. The typical operating mechanism of PDLC is based on the switching of the orientations of LC molecules inside the LC droplet in order to manipulate match or mismatch between the refractive index of LC droplets and of polymer matrix [17–28]. When the droplet size is around the wavelength of incident light, Rayleigh scattering is strong. Thereafter, the polarization independent optical phase exists only when the LC molecules tilts up near parallel to the applied electric fields with random orientations [17]. When the droplet size is smaller than the wavelength of incident light, PDLC is a polarization independent phase modulators due to elimination of Rayleigh scattering [17, 20]. The polymer matrix supporting the LC droplets not only helps speeding response time, but also enlarges the cell gap tolerance under external finger touches. In addition, the optical phase shift of PDLC is polarization independent which also means polarizer-free [17–28]. The optical phase of PDLC, in general, belongs to one of an optically isotropic liquid crystal (OILC) phase modulations as long as PDLC is operated in the pure optical phase region as the voltage is larger than certain bias voltage (V_b). Recently, Niziol reported the Kerr effect of PDLC which means the birefringence of PDLC can be induced under external electric fields, not just orientational birefringence [29]. Therefore, an interest arises from studying the optical phase of PDLC, especially when the droplet size is smaller than wavelength of incident light. In this paper, a study of polarization independent and electrically tunable optical phase of nano liquid crystal droplets dispersed in polymer matrix is investigated. Such an optical medium is optically isotropic and it is so-called an optically isotropic liquid crystals (OILC). We not only discuss the optical theory of the polarization independent phase modulation of OILC, but also demonstrate polarization independent microlens arrays based on the OILC. The experimental results and analytical discussion show that the polarization independent optical phase of OILC microlens arrays results from mainly orientational birefringence which is much larger than the electric-field–induced birefringence (or Kerr effect). The impact of this study can help to design polarization independent LC phase modulations for the applications of light field imaging systems, 3D integrating imaging systems and devices for augment reality.

2. Operating principle and sample preparation

Figures 1(a), 1(b) and 1(c) illustrate the structure and operating principle of OILC phase modulation and OILC microlens arrays. The nano size of droplets is smaller than the wavelength of light. The unpolarized light propagating along + z-direction ($\vec{E}_i$) can be expressed as:

$$\vec{E}_i = A_x \cdot \hat{x} + A_y \cdot \hat{y}, \tag{1}$$

where A_x and A_y are complex numbers. $\hat{x}$ and $\hat{y}$ are unit vectors along x and y axes. Assume n_o and n_e are the ordinary refractive index and the extraordinary refractive index of LC host, respectively. At V = 0, the LC droplets are randomly oriented and the refractive index of the

#240077 Received 30 Apr 2015; revised 8 Jun 2015; accepted 22 Jun 2015; published 24 Jun 2015

OILC is $n_{ave}(V = 0)$ equals to $(2n_o + n_e)/3$ for unpolarized light, as shown in Fig. 1(a). The light propagates out of OILC ($\vec{E}_{out}(V = 0)$) is:

$$\vec{E}_{out}(V = 0) = \vec{E}_i \cdot e^{ik \cdot d \cdot F \cdot (2n_o + n_e)/3}, \quad (2)$$

where k is the wave number, d is the thickness of OILC layer, and F is the filling factor which is the ratio of the droplet volume to the total OILC volume. In Fig. 1(b), when the applied voltage exceeds the threshold voltage (V_{th}), the LC molecules inside the droplet are reoriented by the electric fields because the electric energy is large enough to overcome the anchoring energy of the droplet boundary and internal elastic free energy of LC molecules. The incident light sees an average refractive index of $n_{ave}(V)$. The light propagates out of OILC ($\vec{E}_{out}(V \geq V_{th})$) is:

$$\vec{E}_{out}(V \geq V_{th}) = \vec{E}_i \cdot e^{ik \cdot n_{ave}(v) \cdot d \cdot F}. \quad (3)$$

Under high voltage, the LC molecules inside LC droplet are perpendicular to the glass substrate in Fig. 1(b) and the refractive index for the incident light is $n_{ave}(V) \sim n_o$. From Eq. (2) and (3), the optical phase of OILC is polarization independent and total optical phase shift δφ between a high voltage and V = 0 is up to $k \cdot d \cdot F \cdot (n_e - n_o)/3$. When an inhomogeneous electric field is applied to the OILC using a hole-patterned electrode (Fig. 1(c)), light propagates through OILC and experiences polarization-independent optical phase with a spatial distribution. When such a spatial distribution of optical phase is parabolic, the focal length (f) of the OILC microlens arrays in Fig. 1(c) is [3]:

$$f = \frac{\pi \cdot r^2}{\lambda \cdot \Delta\delta}, \quad (4)$$

where r is radius of the aperture of each sublens and Δδ is the phase difference between the rim and the center of the aperture. The maximum Δδ equals to $\delta\varphi = k \cdot d \cdot F \cdot (n_e - n_o)/3$.

To prepare the sample of the microlens with OILC in Fig. 1(c), we chose the two substrates where the top substrate was only coated with aluminum (Al) metal and the bottom substrate had a planar ITO (indium tin oxide) electrode on the inner side. The Al top substrate was etched with holes. The cell gap and the diameter of holes were 50μm and 100μm, respectively. We then mixed nematic LC (Merck, MLC-2053, Δn = 0.235), NOA65 (a UV curable prepolymer, Norland) and photo-initiator (Irgacure 66) at a weight percent ratio of 44.55:54.46:0.99 at 25 **°C**. The mixture was filled between substrates and then the cell was exposed to UV light at 26 **°C** with an intensity of 200mW/cm^2 for 1 minute. After photo-polymerization, the cell was maintained at 26 **°C** for another 40 minutes for stabilization. To measure the optical phase for discussion, we also prepared an OILC sample in Fig. 1(a) under the identical fabrication process, but the materials are sandwiched between two planar electrodes with the cell gap of 20 μm.

3. Experiment results and discussion

Figure 2(a) shows the SEM (Scanning Electron Microscopy) image of the OILC sample after we removed LC away using hexane. From Fig. 2(a), OILC sample is indeed made up LC droplets dispersed in polymer matrix. The average LC droplet size is ~250 nm. We calculate the filling factor from SEM image by using software called Image J which is a Java-based image processing program developed at the National Institutes of Health. The average filling factor is around 18.3% which indicates area of LC droplets is~18.3% of OILC sample. To measure the transmittance as a function of applied voltage, an unpolarized laser diode (λ = 633nm) was used as a light source, and a photo detector was placed 25 cm behind the OILC sample with planar electrodes to record the light intensity at the different applied

#240077 Received 30 Apr 2015; revised 8 Jun 2015; accepted 22 Jun 2015; published 24 Jun 2015

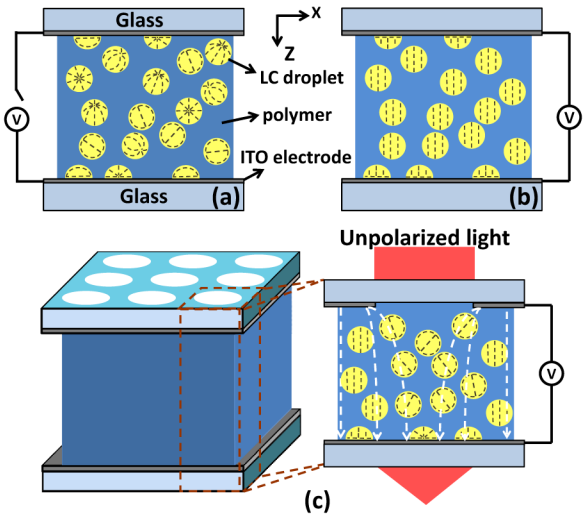

Fig. 1. Schematic diagrams of OILC at (a) voltage-off state and (b) voltage–on state. (c) The structure of OILC microlens arrays. White dotted lines stand for the electric fields.

voltages. The result is shown in Fig. 2(b). To calibrate the transmittance, a cell with the same cell configuration was also prepared which filled with LC (Merck, MLC-2053) only. In Fig. 2(b), the transmittance increases with the applied voltage ranging from 0.73 to 1 as the applied voltage exceeds threshold voltage (V_{th}) of 18 V_{rms}. This is because the small size of randomly oriented LC droplets (~250 nm) results in small scattering and a small mismatch of refractive indices between LC molecules and polymer matrix at V = 0. At a higher voltage, LC droplets are reoriented by the applied electric fields. Such a mismatch of refractive indices between LC molecules and polymer matrix reduces and then transmittance increases up to 1. Compared to the result reported by J. Qi et. al. [28], the threshold electric field of H-PDLC was approximately ~20 V_{rms}/μm, which is higher than ours ~0.9 V_{rms}/μm. This is because the droplet size of our sample is approximately 250 nm which is larger than the results reported by J. Qi et. al.(~100 nm). For smaller LC droplets, the LC inside droplets are more unlikely to re-orientate due to the confinement of polymer network or matrix.

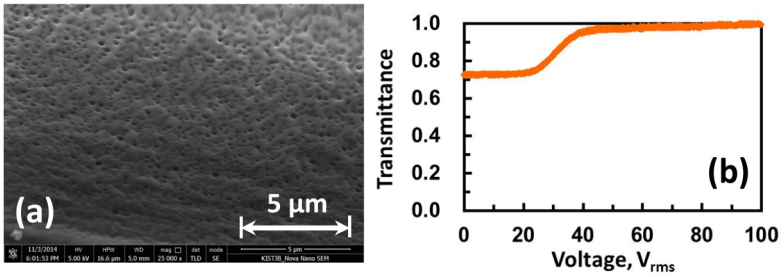

Fig. 2. (a) SEM image of OILC sample. The droplet size is ~0.25 micron. (b) Voltage-dependent transmittance of the OILC sample whose configuration is depicted in Fig. 1(a).

In order to further investigate the phase shift of the same OILC sample, we adopted a Mach-Zehnder interferometer for the measurement of optical phase shifts. An unpolarized He-Ne laser (JDSU, Model 1122, λ = 633 nm) was split into two arms by a beam splitter, and then two beams re-combined again by another beam splitter. The interference fringes were observed when two beams were overlapped. The sample was put in one arm of the interferometer. The fringes were recorded by a digital camera (SONY, DCR-HC40). Figure 3(a) shows the interference fringes at V = 0 and 90 V_{rms}. The visibility is defined as a ratio of

#240077 Received 30 Apr 2015; revised 8 Jun 2015; accepted 22 Jun 2015; published 24 Jun 2015

(I_{max}-I_{min}) to (I_{max} + I_{min}), where I_{max} and I_{min} are the maximum and minimum irradiances of the fringes. In Fig. 3(a), the visibility is 0.74 at V = 0 and 0.78 at V = 90 V_{rms}. High visibility (~0.8) of the interference patterns means the scattering of OILC sample is small. Figure 3(b) also plotted visibility as a function of voltage. The visibilities of OILC sample are ~0.8 at different voltages. This means the sample has small scattering and almost pure optical phase. The reason why the visibility is less than 1 is because of the coherent properties of laser. In addition, we observed the displacement of fringes. By recording the shifted fringes of the OILC sample as the voltage was on and off, we converted the displacement of the fringes to the optical phase shift. Figure 3(b) also plotted the phase shift as a function of applied voltage. From Fig. 3(b), the phase shift increases from 0 to 0.96 π radians as 18 V_{rms} <V< 65 V_{rms}. The phase shift saturates ~0.96 π radians after V> 65 V_{rms}. This is mainly because the LC molecules inside the droplets are almost reoriented perpendicularly to the glass substrates as V> 65 V_{rms}. In Fig. 2(b), the optical phase of the OILC sample is indeed polarization independent under the unpolarized light. In the conventional PDLC, it only has optical phase till the tilt angles of LC droplets are high enough to suppress the scattering as well as all droplets have same tilt angle dispersed along random orientations. As a result, optical phase exists when the voltage exceeds certain high bias voltage (V_b>>V_{th}) [17]. On the contrary, the OILC sample has optical phase shift up to ~π radians as long as V> V_{th}, not V_b. We attribute the large optical phase of OILC to the usage of all the re-orientations of LC molecules, despite of the small droplet size of OILC.

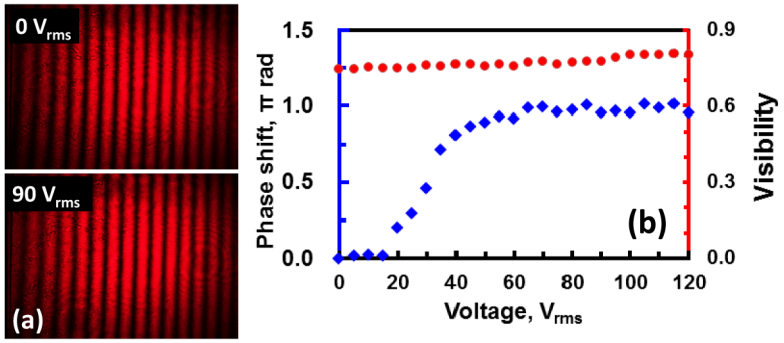

Fig. 3. Interference fringes of OILC sample at (a) V = 0 and V = 90 V_{rms}. (b) Visibility (red dots) and measured phase shift (blue diamonds) of the OILC at different voltages. The cell gap was 20 μm.

In order to demonstrate that the polarization independent optical phase of OILC sample is useful, we fabricated the OILC microlens arrays and characterize the focal length of the sample. To measure the focal length of the OILC microlens arrays, the unpolarized laser (5mW, λ = 633nm) was used as a light source. The laser beam was first collimated by a spatial filter and a solid lens for adjusting the image size. Then the OILC microlens arrays were placed between the spatial filter and the solid lens. A charge-coupled device (CCD) was used to capture the images after the solid lens. We adjusted the location of the sample till we saw the clear aperture image of the sample and then recoded the location. Thereafter, we readjusted the location of the sample while we applied an AC voltage to the sample (square-wave and frequency: 1 kHz) till the sharpest focusing spots were observed at CCD and then recorded the new location. The distance between those two locations was the focal length of the sample at a voltage. Figure 4 depicted the measured focal length as a function of applied voltage. When V> 50V_{rms}, the focal length increases gradually and then decreases with an increase of the applied voltage. The focal length is polarization independent and ranges from 3.4 to 3.8 mm. The bars in Fig. 4 indicate the depth of focus (or DOF) at different voltages. The depth of focus of the OILC lens arrays can help integrate 3D images in integrating image system which is especially important for augment reality [2, 16]. In Fig. 4, DOF is larger as

#240077 Received 30 Apr 2015; revised 8 Jun 2015; accepted 22 Jun 2015; published 24 Jun 2015

$V<120V_{rms}$ (i.e. electric field is $2.4V_{rms}/\mu m$) and is smaller as $V>120V_{rms}$. This might be small scattering and imperfect phase profiles of the microlens arrays as $V<120V_{rms}$ that results in the broaden focal spots and then affects the DOF. Response time of the OILC microlens arrays is around 5.3 ms, which is a summation of the rise time of 0.9 ms and the decay time of 4.4 ms at room temperature. To characterize the focusing properties, the images at CCD were recorded when OILC microlens arrays was placed at 2.95mm away from the position where clear aperture image was acquired. The recorded images at V = 0 V_{rms} and V = 90 V_{rms} are shown in Fig. 5(a) and 5(b). At V = 0 V_{rms}, no focus was observed. At V = 90 V_{rms}, OILC microlens arrays show clear focal spots. Without applied voltage, the low transmittance of the light was contributed by Fresnel diffraction by the small aperture size. With an applied voltage, the OILC microlens arrays show focusing effect. In AR application, the power consumption is key consideration rather than operating voltage. The power consumption of OILC lens array is low due to low electric current that flows through the OILC lens array (~μA) [13]. As to another application of 3D integral imaging system, the large tunable depth of field (DOF) is attractive for reconstructed better images by recording more information at different object planes. To improve the power consumption, lower the driving voltage is way to go by adopting better materials. To enlarge range of tunable DOF, the optical phase of the OILC lens array should be enlarged [15, 16].

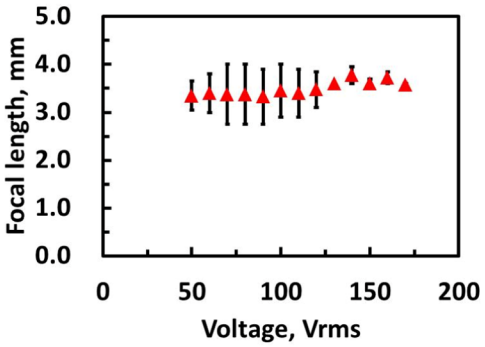

Fig. 4. The focal length of the OILC microlens arrays as a function of an applied voltages under an unpolarized light. (λ = 0.633nm)

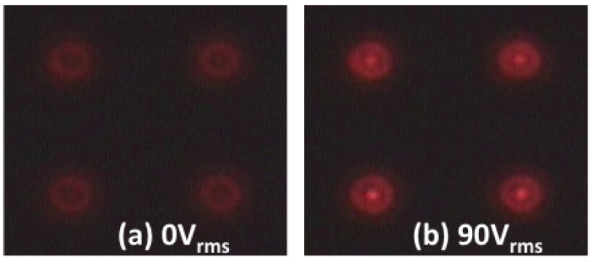

Fig. 5. Measured CCD images of 2D microlens arrays at (a) 0 V_{rms} and (b) 90 V_{rms}.

From the experimental results in Figs. 2 and 3, the maximum phase shift is 0.96 π radians. We can calculate the maximum phase shift by the relation of $\delta\varphi = k \cdot d \cdot F \cdot (n_e - n_o)/3$. The calculated δφ should be 0.91π radians after putting the parameters: λ = 0.633μm, d = 20μm, and F = 0.183. The experimental result is smaller than theoretical result. The possible reason is that the LC molecules are not fully reoriented due to strong anchoring energy from interface between LC and polymer matrix. Another possible reason is that the small deformation of LC droplet due to the strong electric fields results in elongated optical path. As a result, the optical phase in experiment is larger than the theoretical one. According to Eq. (4), the

#240077 Received 30 Apr 2015; revised 8 Jun 2015; accepted 22 Jun 2015; published 24 Jun 2015

calculated phase shift from the deduction of focal length (~3.6 mm in average) is around 1.097 π radians. We further calculate ($n_{ave}(V)-(2n_o + n_e)/3$) ~0.113 from Eq. (2) and Eq. (3). This indicates the distribution of electric fields is not good enough to reach the birefringence of LC host to obtain maximum phase shift (i.e. $\Delta\delta << \delta\varphi$ in Eq. (4)). To enlarge the phase of the OILC microlens arrays, we can increase the droplet size or filling factor, and optimize the aperture size. Owing to the transverse electric fields around the edge of the aperture in Fig. 1(c), Kerr effect can also contribute the optical phase to the OILC microlens arrays [29, 30]. The Kerr effect of PDLC has been reported in a literature [29]. Assume the birefringence of Kerr effect is Δn_{Kerr} which satisfies the relation: $\Delta n_{kerr} = \lambda \cdot K \cdot E^2$, where K is Kerr constant and E is electric field. We then measured Kerr constant by tilting the sample 5, 10, and 15 degree with respect to the incident light [31]. The measured Kerr constant is around $4.78 \times 10^{-9} mV^{-2}$ as the electric field is 3V/μm. As a result, the electric-field induced birefringence Δn_{Kerr} is around 0.027 which is much smaller than 0.113 resulting from the change of LC orientations of refractive index. Therefore, the optical phase of the OILC microlens arrays mainly originates from LC orientation inside the droplets.

4. Conclusion

We discussed polarization independent and electrically tunable optical phase of nano liquid crystal droplets dispersed in polymer matrix which is optically isotropic. We also demonstrate polarizer-free and fast response microlens array based on optical phase modulation of OILC. The focal length of the OILC microlens arrays is about 3.4 mm at $90V_{rms}$ and response time is about 5.3 ms. The polarization independent optical phase of the OILC microlens arrays results from mainly orientational birefringence which is much larger than the electric-field–induced birefringence (or Kerr effect). The tunable phase shift and the transparency are higher than published microlens arrays using PDLC [17]. In AR application, polarization independent lens arrays with fast response time and tunable focal length could be used as extra phase compensation elements to compensate internal aberrations due to manufacture of the systems or to add extra optical phase for adapting eye conditions of users. The potential applications are light field imaging systems, 3D integrating imaging systems and augment reality.

Acknowledgments

This research was supported partially by the National Research Foundation (NRF) Korea, the Korea-China Joint Research Program under grant No.2012-0004814 and partially by Department of Natural Sciences and Sustainable Development in Ministry of Science and Technology (MOST) in Taiwan under the contract no. NSC 101-2112-M-009 –011 -MY3.

#240077 Received 30 Apr 2015; revised 8 Jun 2015; accepted 22 Jun 2015; published 24 Jun 2015